Nanostructured Silver-Based Surfaces: New Emergent Methodologies for an Easy Detection of Analytes

Maria Staiano,[†] Evgenia G. Matveeva,[‡] Mauro Rossi,[§] Roberta Crescenzo,[†] Zygmunt Gryczynski,[‡] Ignacy Gryczynski,[‡] Luisa Iozzino,[†,||] Irina Akopova,[‡] and Sabato D'Auria*[,†]

Laboratory for Molecular Sensing, Istituto di Biochimica delle Proteine—Consiglio Nazionale delle Richerche, Naples, Italy, Center for Commercialization of Fluorescence Technologies, Department of Molecular Biology and Immunology, University of North Texas, Health Science Center, Fort Worth, Texas, Institute of Food Sciences, Consiglio Nazionale delle Richerche, Avellino, Italy, and School of Veterinary Medicine, University of Naples Federico II, Naples, Italy

ABSTRACT In this work, we describe how to realize a new sensing platform for an easy and fast detection of analytes. In particular, we utilized enhanced fluorescence emission on silver island films (SIFs) coupled to the total internal reflection fluorescence mode (TIRF) to develop a new assay format for the detection of target analytes. Here, as an example, we report on the detection of the toxic peptides present in gliadin (Gli). Our assay was performed as follows: (1) gliadin was first captured on surfaces coated with anti-Gli antibodies; (2) the surfaces were then incubated with fluorophore-labeled anti-Gli antibodies; (3) the signal from the fluorophore-labeled anti-Gli antibody bound to the antigen was detected by TIRF. The system was examined on glass surfaces and on SIFs. We observed a relevant enhancement of the signal from SIFs compared to the signal from the glass substrate not modified with a SIF. In addition, the estimated detection limit (EDL) of our methodology was 60 ng/mL (or lower). This limit is therefore lower than the clinical cut-off for Gli presence in food for celiac patients. The advantage of our method is a reduced number of testing steps, which allows for easy detection of residual toxic peptides in food labeled as gluten free. The proposed technology can be easily expanded to the determination of different target analytes.

KEYWORDS: celiac disease • fluorescence assay • gliadin immunoassay • silver island films • total internal reflection fluorescence

INTRODUCTION

Celiac disease (CD; other abbreviations: area under the curve, AUC; estimated detection limit, EDL; front face, FF; gliadin, Gli; radiative decay engineering, RDE; reversed-phase HPLC, RP-HPLC; surface-enhanced Raman scattering, SERS; silver island film, SIF; total internal reflection fluorescence, TIRF; tissue transglutaminase, tTG) is an immune mediated disease of the small intestine affecting genetically susceptible people following feeding with wheat gluten and related proteins from barley and rye (1, 2). In particular, gluten is composed of two classes of proteins: gliadins, soluble in aqueous alcohols, and insoluble glutenins. Gliadin proteins are primarily responsible of CD. Reversed-phase HPLC (RP-HPLC) can separate gliadin into more than 30 components according to their polarity in ω-, α-, and γ-gliadins (3). The high content of proline residues makes gliadins very resistant to gastric, pancreatic, and intestinal proteases. This stability can play a role in the immune reactivity of gluten proteins (4). Another crucial biochemical issue involved in the pathogenesis of CD is the deamidation of specific glutamine residues of gliadin, a reaction catalysed by tissue transglutaminase (tTG) (5) that increases the ability of gliadin peptides to elicit a T-cell response (6). Taken together, these features underscore the main difficulties in developing immunoassays that are able to determine the exact content of gluten in food, especially at very low doses, in an easy way. The essential need for such methods is highlighted by the consideration that a strict gluten-free lifelong diet is mandatory for celiac patients for the recovery of the mucosal lesion. Nevertheless, full adherence to diet is often hampered by the very low amount of gluten required to induce the disease. In addition, unintentional gluten uptake can often occur through ingesting food considered gluten-free. Until now, none of the produced methods are considered to be fully adequate.

Different enzyme-linked immuno-sorbent assays (ELISAs) have been developed so far to determine the gliadin content in food. Some of them are based on the detection of the heat-stable ω-gliadin (7) whose content in the gliadin mixture is quite variable, depending on the different cultivars. More

* Correspondence to: Dr. Sabato D'Auria, Laboratory for Molecular Sensing, IBP-CNR, Via Pietro Castellino, 111, 80131 Napoli, Italy, Tel: +39-0816132250, Fax: +39-0816132277, E-mail: s.dauria@ibp.cnr.it.

Received for review September 11, 2009 and accepted December 02, 2009

[†] Laboratory for Molecular Sensing, Istituto di Biochimica delle Proteine—Consiglio Nazionale delle Richerche.

[‡] University of North Texas.

[§] Institute of Food Sciences, Consiglio Nazionale delle Richerche.

[||] University of Naples Federico II.

DOI: 10.1021/am900617p

recently, a sensitive quantitative ELISA, based on the detection of a gluten-related penta-peptide, has been developed (8). Nevertheless, the usefulness of such immuno-assays for CD patients is still under debate: essentially, both systems are not strictly related to the detection of known toxic sequences (9−11).

The applications of surface plasmon enhancement of fluorescence on surfaces coated with metal nanoparticles are very promising (12−18). Metal (silver) nanoparticles can be synthesized in solution by silver cations reduction (19−26), and then deposited onto the surface. Alternatively, silver nanoparticles can either be generated or grown directly on the surface by laser reduction (27), wet chemical reduction such as Tollen reaction (14−17, 28), or thermal silver evaporation (29−31).

The process of fluorescence enhancement near silver nanoparticles has been known for several decades (32, 33). There are two general factors responsible for the enhancement. The first is an enhanced local field generated near metallic nanoparticles. Colloidal and rough metallic particles are also used in a surface enhanced Raman scattering (SERS) (34, 35), where the local light fields are many-fold enhanced. The second factor is an interaction of the excited molecule with metallic nanoparticles, the effect known as radiative decay engineering (RDE) (36). The rapid transfer of the excitation to the metallic nanoparticle is followed by the far field radiation. This effect increases molecules' brightness and decreases the lifetime (this is only possible if the radiative rate of deactivation increases). The total enhancement is a product of these two effects, the enhanced local field and RDE. It should be noted that at short distance between fluorophore and SIF distances, below 5 nm, the fluorescence is quenched. The optimum distance between fluorophore and SIF is estimated to be about 10 nm (37).

In the present work, we utilized the method of enhanced fluorescence on silver island films (SIFs) coupled to the total internal reflection mode (TIRF) to detect the presence of gliadin. We treated mice on a gluten-free diet for several generations and produced high-avidity anti-gliadin antibodies. These antibodies were applied in an immunoassay to detect toxic gliadin. The estimated detection limit (EDL) of our methodology is 60 ng/mL (or lower) that represents the clinical cut-off for Gli presence in food for celiac patients (8). There is no need for washing steps: this is an advantage of our method, which allows for a simpler test to detect residual gluten in food for celiac patients.

The proposed technology can be easily expanded to the determination of different target analytes.

MATERIALS AND METHODS

Reagents. A Rhodamine Red-X antibody labeling kit was purchased from Invitrogen. Seta-670 mono-NHS ester (catalog # K8-1342) was kindly donated by SETA BioMedicals, Urbana, IL. Salts and other buffer components (such as Tween-20), bovine serum albumin, glucose, sucrose, and $AgNO_3$ were purchased from Sigma-Aldrich. Microscope glass slides were purchased from VWR, 3×1 inch and 1 mm thick.

Preparation of Slides Coated with Silver Island Films (SIFs). SIF surface was formed according to the procedure described elsewhere (14, 15). Briefly, half of the surface of each slide was modified by depositing SIF by chemical reduction of silver nitrate by wet-chemical process using D(+)glucose. The remaining half of each slide was left unmodified and used as a control (bare glass).

Generation of Polyclonal Mouse Anti-Gliadin Antibodies. BALB/c mice from a colony reared on a gluten-free diet were used for generating gliadin-specific antibodies. These mice are devoid of pre-existent oral tolerance to gliadin and develop higher specific IgG titers than mice fed a standard diet (7). The immunogen we used was wheat gliadin, extracted from a commercial preparation (Sigma Chemical Co., St. Louis, MO) with 70 % (v/v) ethanol and freeze-dried. All gliadin components are present in the preparation. Groups of mice ($n = 6$) were immunized intra-peritoneally with 50 μg of gliadin emulsified in Freund's complete adjuvant. Mice were boosted twice after 2.5 and 5 weeks with 50 μg of gliadin emulsified in Freund's incomplete adjuvant. Serum was collected after a further 1.5 weeks. IgG were purified by affinity chromatography by using an Affi-Gel Protein A MAPS II kit (Bio-Rad Laboratories, Hercules, CA, USA) according to the manufacturer's instructions. Western blot analysis indicated that all the gliadin components (α-, γ-, and ω-fractions) were recognized by the purified antibodies (data not shown).

Preparation of Gliadin Samples. Gliadin samples were extracted from flour according to the Osborne fractionation procedure (38). Briefly, 100 grams of flour was resuspended in 100 mL of 0.4 M NaCl in 67 mM NaH_2PO_4, pH 7.6, and extracted by shaking for 10 min; after centrifugation at 15 500 g for 15 min, the pellet was recovered and extracted with 20 ml of 70 % ethanol in water by shaking for 45 min at 50°C; after centrifugation at 15 000 g for 15 min, the supernatant containing the gliadin fraction was recovered, freeze-dried, and stored at −20°C.

Preparation of a Peptic/Tryptic Digest of Prolamins. 40 mg gliadin samples were resuspended in 0.4 mL of 0.1 N HCl pH 1.8 with pepsin (protein:enzyme 100:1) at 37°C for 4 h in a shaking bath. The pH was then raised to about 8.0 using 2N NaOH. Trypsin was then added (protein:enzyme = 100:1) and the reaction performed at 37°C for a further 4 h; the reaction was stopped by incubating in boiling water for 10 min. Samples were freeze-dried and stored at −20°C.

Labeling of Antibodies. Reporter antibodies were labeled with Rhodamine Red-X using a labeling kit from "Invitrogen". The kits provided the dye with reactive succinimidyl ester moiety, which reacts effectively with the primary amines of antibodies. The dye/protein ratio in the conjugate (after chromatographic separation of unbound dye using elution with 50 mM Na-phosphate buffer, pH 7.3) was determined by the spectrophotometer according to the kit instructions: dye concentration was determined from the visible part of the spectra, using the published molar extinction coefficient ($\varepsilon_{570} = 120\,000$ cm^{-1} M^{-1} for Rhodamine Red-X), and the antibody concentration was determined from the UV part of spectra ($\varepsilon_{280} = 203\,000$ cm^{-1} M^{-1} for IgG), taking into account the UV absorbance contribution from the covalently bound dye ($0.17A_{570}$ for Rhodamine Red-X), where A_{570} is absorbance at 570 nm). The dye/protein ratio in the purified conjugate was 3.0.

The labeling of the reporter antibodies with the label Seta-670 (NHS ester) was performed similarly. The dye/protein ratio in the conjugate was determined spectrophotometrically using the molar extinction coefficient ($\varepsilon_{667} = 179\,000$ cm^{-1} M^{-1} for Seta-670, see ref 39) and the correction procedure described below. UV absorbance contribution from the covalently bound dye in the antibody conjugate was determined by measuring the absorbance spectra of the free dye and found to be $0.086A_{667}$, where A_{667} is absorbance at 667 nm. The visible absorption spectra for this dye−IgG conjugates are different from the spectra of the free unconjugated dye: depending on

the dye/protein ratio, the shape of the peak alters and a second absorption band appears (40). Therefore, we used a correction procedure for the visible portion of the spectra: we used the integrated area under the visible part of the spectrum (AUC) for quantization of the dye in the conjugate instead of the height of the dye peak (40). We previously calculated the correction factor of our conjugate in order to correct the peak height. This correction factor was equal to the ratio of the AUC for the conjugate to the AUC for the free non-conjugated label. The spectra were normalized to the height of the free dye peak). The dye/protein ratio in purified conjugate was 10.

Gliadin Assays. Gliadin immunoassays were performed in a "sandwich" format. Briefly, slides (covered with the tape containing punched holes, circles 6 mm in diameter each) were non-covalently coated with the captured anti-gliadin (anti-Gli) antibody (50 μg/mL in 50 mM sodium phosphate buffer, pH 7.3, incubation at room temperature overnight). We then blocked the residual binding sites: 2 h incubation at room temperature with blocking buffer, 1% bovine serum albumin, 1% sucrose, 0.05% NaN_3, 0.05% Tween-20 in 50 mM Na-phosphate buffer, pH 7.3. Next, we added gliadin at a concentration of 5 μg/mL (the Gli solution was diluted with a blocking buffer from a stock gliadin solution of 10 mg/mL in 75% aqueous EtOH or 10 mM AcOH). We used the blocking buffer without gliadin as a blank control sample. After an incubation period (1 h at room temperature) and a washing, a conjugate of the labeled reporter anti-Gli antibody with Rhodamine Red-X or Seta-670 was added (at 5 μg/mL in blocking buffer), followed again by incubation (1 h at room temperature). We then measured the resulting emission fluorescence signal (the assay without the washing step, in the presence of an excess of the non-bound labelled antibodies). For the assay with washing step, the supernatant (the excess of the non-bound labeled secondary antibodies) was removed; the slide surface was rinsed with water, washing solution (0.05% Tween-20 in water), and water again, and then covered with 50 mM sodium phosphate buffer, pH 7.3; fluorescence signal was measured after this procedure. Albumin was used as a control in both of the above experiments.

The estimation of the detection limit (EDL) was calculated from the signal produced by the blank sample plus 3 SDs (standard deviations), based on the measurements of 12 blank signals taken during 3 different experiments (different days, slides, antigen stock solutions). To translate the results into analyte concentration units, we applied a linear trend based on one concentration we used and average blank signal. On the basis of our previous experiments (data not shown), we believe that the accurate calibration curve in this concentration range is not all linear: it is linear only at low concentrations and becomes exponential at higher concentrations. Therefore, when measured accurately using the low-concentration range dose-response curve, we expect the limit of detection to be significantly lower.

Spectroscopic Measurements. The solution and slide surface absorption spectra were measured using a Varian Cary Eclipse spectrophotometer (Varian Analytical Instruments, USA). We measured the fluorescence of the samples on the glass and glass-SIF slides by placing the slides horizontally on the total internal reflection setup (Figure 1). The TIRF setup consisted of a coupling prism mounted in the custom-made holder. For excitation, we used small solid-state laser diodes (532 nm, used for commercial laser pointers). The sample in a 6 mm diameter well was illuminated in the center by an evanescent field spot, about 1 mm in diameter. The emission spectra were collected by an optical fiber, 4 mm thick, mounted on a x and y positioner about 2 mm from the sample. The other end of the 5-foot-long fiber was directed to a Varian Cary Eclipse fluorometer (Varian Analytical Instruments, USA). The 550 nm long wave pass filter was used to reject the scattering 532 nm excitation light.

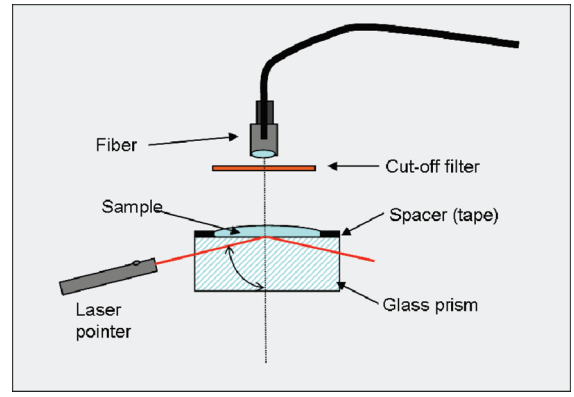

FIGURE 1. Optical scheme illustrating the geometry for the total internal reflectance fluorescence measurements performed in the work. Experimental details are reported in Materials and Methods.

AFM. Atomic force microscopy (AFM) images were collected by scanning dry sample slides (14) with an atomic force microscope (TMX 2100 Explorer SPM, Veeco), equipped with AFM dry scanner. The AFM scanner was calibrated using a standard calibration grid as well as 100 nm diameter gold nanoparticles, from Ted Pella. The images were analyzed using SPMLab software.

RESULTS AND DISCUSSION

Antibodies and Antigen. High-affinity antibodies were raised in mice reared for several generations on a gluten-free diet. Under these conditions, mice do not develop immunological tolerance to the food antigen gliadin; consequently, parenteral immunization elicits a much higher specific IgG titer. As another weakness of the gluten analysis is represented by the low solubility of gliadin in hydrophilic buffers, extracted gliadin samples were subjected to enzyme digestion with pepsin and trypsin. Digested gliadin samples were then used for immunoassay experiments. The validation of specificity of the produced antibodies was made by testing the different digested ethanol soluble protein samples extracted from both toxic (wheat, barley rye) and non-toxic (corn and rice) cereal flours (41). ELISA data confirmed the high specificity of the produced antibodies that were able to recognize gliadin cross-reactivity at very high sample dilutions only in toxic cereals (41). Western blot analysis confirmed that all the gliadin components (α-, β-, γ-, and ω-fractions) can be detected by these polyclonal antibodies. Considering that T-cell stimulatory epitopes for CD have been identified in all these proteins (42), our data highlighted the value of raised antibodies. Moreover, the high specificity for gliadin was confirmed by the finding that no cross-reactivity with albumin, globulin, and glutenin wheat fractions was observed (data not shown). Importantly, cross-reactivity with ω-gliadin, which did not present differential heat stability (43), also suggested a specificity of antibodies for the analysis of samples extracted from baked food.

These antibodies were used in this work for the detection of Gli by a methodology based on the utilization of silver islands coupled to fluorescence emission, namely, enhanced-fluorescence linked immuno-sorbent assay (EFLISA) (Figure 2).

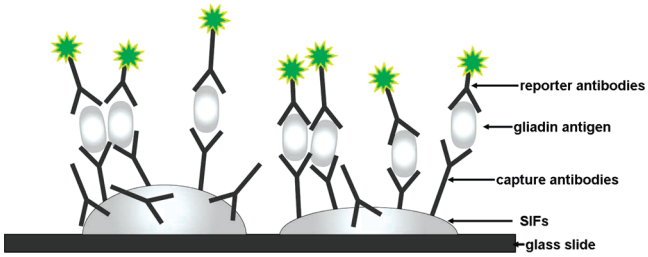

FIGURE 2. Schematic representation of EFLISA methodology for the detection of gluten.

Surface Topography. We performed surface assays on regular size glass microscope slides with and without SIF coating; such glass surface is not optimal for performing EFLISA. The plastic immunoassay 96-well plate provides better surface antibody binding and better assay sensitivity. However, our goal was to compare the gliadin immunoassay utilizing the TIRF detection on SIF-coated surface to the control immunoassay at identical conditions (same reagents, incubation times and temperatures, and detection method) and to demonstrate the signal enhancement due to the SIF coating. We used glass slides because it is very difficult to get stable uniform SIF coating inside the 96-well plate. Figure 3 presents an example of an AFM image of a SIF-coated slide. As we can see from the image (Figure 3A), silver islands vary in height and width even within a small AFM scan area (25× 25 μm). According to the profile analysis (14), the height of the silver islands varies between 25−30 and 80 nm, and the width varies between 140 and 300 nm results (first top, second middle, and third bottom profiles from Figure 3C correspond to vertical blue, horizontal red, and inclined green lines from Figure 3B). Some islands from agglomerates of larger width are also present.

Enhanced Fluorescence on SIFs. Typical examples of the fluorescence spectra from the assay samples in a sandwich format collected from SIF-modified or non-modified glass substrates are presented in panels A and B in Figure 4. Spectra represent labelled anti-Gli antibodies bound to the surface immobilized antigen (Gli bound to the capture anti-Gli Ab). For both conjugates (Rhodamine Red-X labelled or Seta-670 labelled), there is enhancement of the signal on SIF surface, compared to the bare glass surface.

The enhancement ratio was calculated as a ratio of the average signal measured from SIF-modified glass surface to the average signal measured from the non-modified glass surface. This enhancement may depend on numerous factors, such as the density of the SIF, the type of the fluorophore, the wavelengths of the excitation and emission (16), and in our case of the gliadin sandwich assay, it may also depend on the Gli concentration. We optimized the parameters of the experiments by keeping the density of the SIF layer to a reproducible and optimal level following the indications present in ref 17. The absorbance of the coated glass slides was between 0.5 and 1 OD.

Because of large variation in size of the SIF nanoparticles (even at similar average optical density of the SIF-coated slide), we performed averaging in order to calculate the immunoassay signal. The signal for each spot was calculated as the average within 5 nm at maximum emission (signals at maximum ±2.5 nm have been averaged). Next, the fluorescence measurements for each sample were repeated 4−6 times on different spots and the signals were again averaged, and standard deviations (SDs) calculated. Examples of the assay signal in the absence and in the presence of silver islands are shown in Figure 5. The values of the enhancement factor for different SIF batches are presented in Table 1. The sensitivity of the assay is enhanced by a factor of about 5−10 times when the assay is performed in the presence of SIFs. The enhancement factor depends on the SIF surface properties, such as optical density, size, shape, and uniformity of the particles: as we can see from Table 1, it varies widely from 5 to 16 for different SIF batches. We have studied in detail the enhancements of similar model immunoassays (binding of labelled anti-rabbit antibodies to rabbit IgG) on SIFs earlier (16), and we observed similar enhancement values ranging from 4 to 8 (for different SIF batches prepared by the same wet chemistry manual reduction method) for Rhodamine Red-X label. The immunocomplex forming in a model immunoassay (16) consists of two bound IgG's (and not a sandwich of two IgG's with the gliadin antigen in-between as in this work), so there should be a difference in the size of the immunocomplexes and hence the average distance between the fluorophore and metal particles may be slightly larger in case of the gliadin sandwich if compared to the model immunoassay complex. We have also studied earlier the enhancements of the sandwich myoglobin immunoassay by the same SIF surfaces (17), where we typically observed 10−15 enhancement values for Rhodamine Red-X label. It is notable that the sizes of the gliadin sandwich and myoglobin sandwich should be close, taking into account that both antigens are not very large if compared to the IgGs. IgG has a molecular weight of about 150 kD and the size of the native IgG molecule is about 12 × 9 × 5 nm (44). The enhancement zone extends up to approximately 20 nm (14, 45), with a quenching zone very close to silver particles (approximately up to 4 nm) and maximum enhancement peak at approximately 9 nm (45) .Gliadins have molecular weight of about 30−45 kD and myoglobin about 18 kD, and the input of the antigen to the total size of the sandwich is reduced because the antigen is buried inside the binding sites of the IgG's forming the complex. Hence the larger size of the sandwich may be more favorable for the metal-enhanced fluorescence signal, which may explain the slightly higher enhancement values for the sandwich (5−16 for gliadin sandwich in this work, 10−15 for myoglobin sandwich in ref 17) compared to the values of 5−8 in two bound IgG's in ref 16. The immunoassays in this work, 16, and 17 have been performed on SIFs obtained by the same method and in the same experimental conditions (same label, same incubation times and conditions, same washing steps). However, the difference in enhancement values is not large and this hypothesis requires additional research.

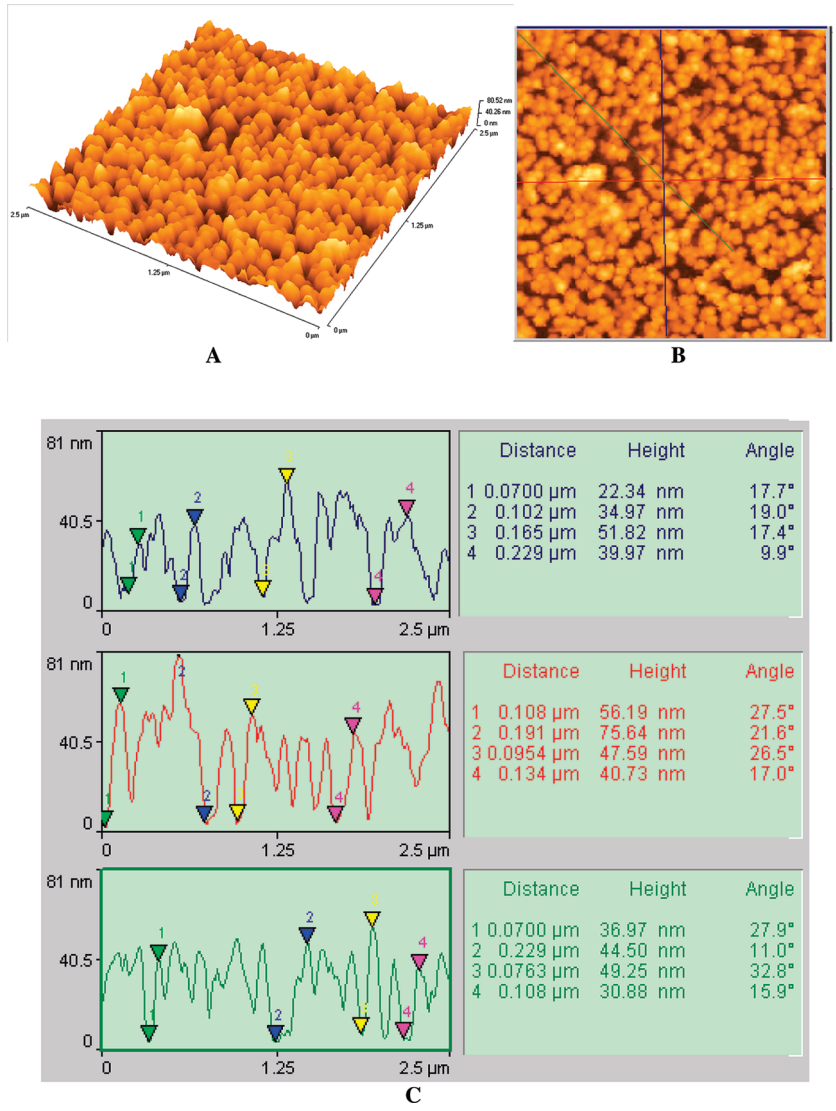

FIGURE 3. AFM surface topography of a SIF-coated glass slide: (A) 3D image (25 × 25 μm^2); (B) same 2D image showing three profile lines; (C) profile analysis data.

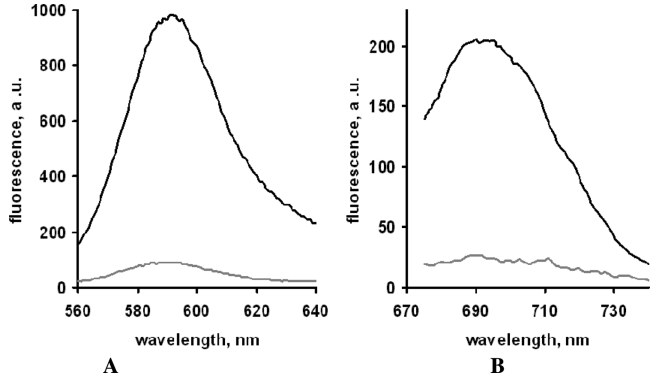

FIGURE 4. Gliadin immunoassay response: emission spectra of (A) Rhodamine anti-gliadin antibodies and (B) Seta anti-gliadin antibodies captured by Gli on the surface in the absence (grey traces) and in the presence (black traces) of silver islands. Immunoassay details are described in Materials and Methods, part "Gliadin assays".

We also estimated the detection limit (EDL) of our methodology for two different SIF batches, with average enhancement factors of approximately 5 and 8 (Table 1). The estimation of the detection limit has been performed from the signal produced by the blank sample plus 3 SDs (standard deviations), based on the measurements of 12 blank signals taken in 3 different experiments (different days, slides, antigen stock solutions). The data shown represent the mean and standard deviation of five different experiments in which different slides and different secondary antibodies were used. To translate it to the analyte concentration units, we applied a linear trend based on one concentration we used and average blank signal. On the basis of our previous experiments (17) for a different protein with comparable molecular weight (myoglobin) at same experimental conditions (on SIF-coated slides in same size wells, at TIRF configuration, using Rhodamine Red-X labeled reporter antibodies with similar dye/antibody ratio) (data not shown), we believe that the accurate calibration curve in this concentration range is not linear: it is linear only at low concentrations and exponential saturation at higher concentrations. Hence, we expect the limit of detection to be

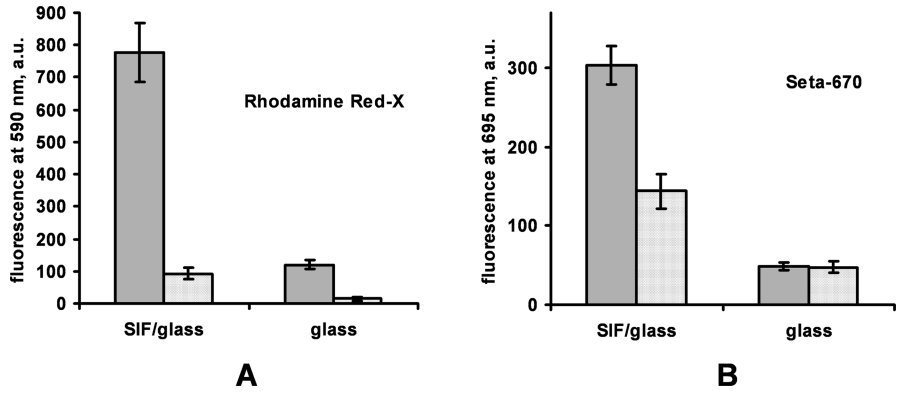

FIGURE 5. Examples of the gliadin assay using (A) Rhodamine or (B) Seta labeled Gli in the absence and presence of silver islands. Grey bars represent the signal in the presence of Gli and white bars represent the signal in the absence of Gli. The temperature was 22° C. The error bars represent the standard deviation calculated for the five different experiments.

Table 1. Fluorescence Enhancement Ratios and EDL Values Measured for Different Batches of SIFs Using RhRed-X Labeled Antibodies

		EDL (ng/mL)	
SIF batch	ratio	SIF/glass	glass only
#1	5.2	59	260
#2	6.5		
#3	8.4	49	220
#4	8.5		
#5	9.9		
#6	14.3		
#7	16.2		

at least several times lower (at least 5−10 times according to data reported in ref 17) when measured accurately using a low concentration range dose-response curve. From Table 1 we see that SIF surface allows an approximately 5-fold improvement in EDL, with the EDL lower than 60 ng/mL. This level results in much lower than EDL from classical gliadin immunoassays; notably, it widely overcome the established detection limit for Gli traces in gluten-free food (8).

Clearly, these manually prepared SIF coatings, as used in our research, cannot be used as-is for commercial devices without a drastic improvement in uniformity of the particles (which should result in much smaller deviations). Highly uniform coatings similar to SIFs are currently not commercially available; such coatings can be custom-ordered from nanolithography facilities. However, a small number of supports (with coated area of only about 1×1 mm^2) would cost several thousand U.S. dollars. Hence, in order to demonstrate the applicability of our methodology to the gliadin detection assay, we used a very fast and cheap manual wet chemistry method for the preparation of the SIF coatings. Gliadin detection in real food samples and an accurate determination of the detection limit should be performed on uniform coatings; this is the topic of our further investigations.

There is a large interpatient variability in the sensitivity to trace intakes of gluten. This feature should be accounted for in the implementation of a safe gluten threshold and a sensitive quantitative assay. Presently, a discrepancy in national positions hampers the realization of uniform international guidelines on the maximum level of gluten contamination (expressed as ppm). In Northern European countries, up to 200 ppm gluten is permitted in food for CD patients. Conversely, a more prudent value of 20 ppm was adopted in North America and Southern Europe. Finnish experts recently supported the intermediate limit of 100 ppm (46). The decision about what the threshold is depends, however, not only on the minimum toxic dose, but also on the amount of gluten-free (GF) products consumed. In accordance with this concept, in vivo micro-challenge studies confirmed that abnormal small bowel morphology persisted in a significant proportion of CD patients being treated with a GF diet, most likely because of the persistent ingestion of trace amounts of glute n (47). This study clearly indicates that a 100-ppm threshold, up to 10 mg gluten/100 g of product, is not suitable, especially in countries where consumption of wheat substitutes is as high as 500 g/day. The threshold of 20 ppm keeps the intake of gluten below the amount of 50 mg/day, which allows a safety margin. But again, the variable gluten sensitivity and patient dietary habits remains to be considered. Taken together, these considerations justify our search for a powerful sensitive assay, which detects residual gluten content in products with higher precision.

In addition to the high sensitivity due to the use of SIFs, our assay is almost independent of the washing (which removes the excess of the labeled antibodies) through TIRF excitation. We performed the assay with or without washing (Figure 6) and compared the two detection modes: TIRF mode and front face (FF) detection. FF detection was performed using excitation from the top of the sample, resulting in the excitation light entering from the top and going through the sample before reaching the surface. The hatched bars represent the assay with a washing step (after removing the excess of the labeled antibodies and washing with buffer). We can see from Figure 6 that the assay signal is approximately the same (within experimental error) with or without the washing step in the TIRF mode. The conventional FF mode results in a high input of supernatant

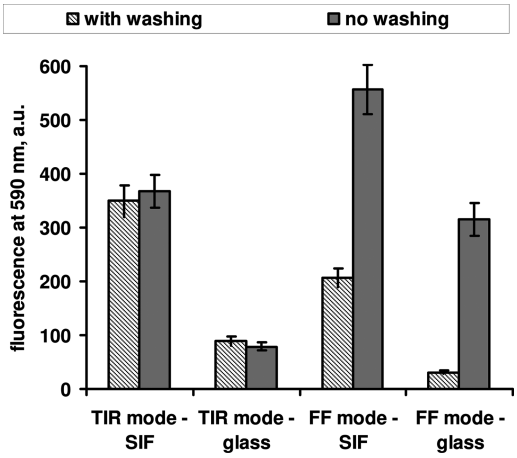

FIGURE 6. Effect of washing steps and optical configuration of the detection of the intensity of fluorescence emission on bare glass and SIF-coated glass surfaces. The temperature was 22° C. The data shown represent the mean and standard deviation of five different experiments. The grey bars represent the assay without the washing step (in the presence of the excess non-bound labelled antibodies) and the hatched bars represent the assay with the washing step (after removing the excess non-bound labeled antibodies and washing with buffer).

fluorescence (nonbound fluorescently labelled secondary antibodies). This background fluorescence exceeds the sample signal many-fold. The ability to measure fluorescence without a washing step is critical for optically dense samples with high background fluorescence, e.g., a food sample matrix.

In conclusion, in this work, we developed a new approach for detection of toxic peptides present in gliadin. The use of silver island films as a sensing platform offers a low detection limit and reproducibility and is practically free of washing steps. Although recently some of us reported higher enhancements on sharp silver nanostructures like fractals than silver island films (48, 49) or self assembled silver colloids on a metallic film (49) we believe that silver island films are more appropriate supports for real assay for gliadin. In fact, this kind of assay requires a high degree of reliability and reproducibility that are ensure by the use of SIFs. On the contrary, we feel that irregular silver nanostructures offer extremely high enhancements in "hot spots" and their use is more appropriate for single-molecule detection studies.

Acknowledgment. This project was realized within the CNR Commessa "Diagnostica Avanzata ed Alimentazione" program. This work was also supported by the ASI project MoMa 1/014/06/0 (MS,SD) and the Texas Emerging Technologies Fund (E.M., Z.G., I.G.). The authors thank Dr. Paolo Bazzicalupo and Ms. Maria Matveeva for the language revision.

REFERENCES AND NOTES

(1) Maki, M.; Collin, P. *Lancet* **1997**, *349*, 1755–1759.
(2) Tursi, A.; Giorgetti, G.; Brandimarte, G.; Rubino, E.; Lombardi, D.; Gasbarrini, G. *Hepatogastroenterology* **2001**, *48*, 462–464.
(3) Wieser, H.; Seilmeier, W.; Belitz, H.-D. Z. *Lebens. Unters. Forsch.* **1987**, *184* (5), 366–373.
(4) Shan, L.; Molberg, O.; Parrot, I.; Hausch, F.; Filiz, F.; Gray, G.M.; Sollid, L. M.; Khosla, C. *Science* **2002**, *297*, 2275–2279.
(5) Molberg, O.; McAdam, S. N.; Korner, R.; Quarsten, H.; Kristiansen, C.; Madsen, L.; Fugger, L.; Scott, H.; Noren, O.; Roepstorff, P.; Lundin, K. E.; Sjostrom, H.; Sollid, L. M. *Nat. Med.* **1998**, *4*, 713–717.
(6) van de Wal, Y.; Kooy, Y.; van Veelen, P.; Peña, S.; Mearin, L.; Papadopoulos, G.; Koning, F. *J. Immunol.* **1998**, *161*, 1585–1588.
(7) Skerrit, J. H.; Hill, A. S. *Lancet* **1991**, *337* (8738), 379–82.
(8) Sorell, L.; Lopez, J. A.; Valdes, I.; Alfonso, P.; Camafeita, E.; Acevedo, B.; Chirdo, F.; Gavilondo, J.; Mendez, E. *FEBS Lett.* **1998**, *439*, 46–50.
(9) De Stefano, L.; Rossi, M.; Staiano, M.; Mamone, G.; Parracino, A.; Rotiroti, L.; Rendina, I.; Rossi, M.; D'Auria, S. *J Proteome Res.* **2006**, *5*, 1241–5.
(10) Staiano, M.; Scognamiglio, V.; Mamone, G.; Rossi, M.; Parracino, A.; Rossi, M.; D'Auria, S. *J Proteome Res.* **2006**, *9*, 2083–6.
(11) Sollid, L. M. *Annu. Rev. Immunol* **2000**, *18*, 53–81.
(12) Barnes, W. L.; Dereux, A.; Ebbesen, Th. W. *Nature* **2003**, *424*, 824–830.
(13) Maliwal, B. P.; Malicka, J.; Gryczynski, I.; Gryczynski, Z.; Lakowicz, J. R. *Biopolymers* **2003**, *70* (4), 585–594.
(14) Lakowicz, Y., Jr.; Shen, Y.; D'Auria, S.; J; Malicka, J.; Z.; Gryczynski, Z.; Gryczynski, I. *Anal. Biochem.* **2002**, *301* (2), 261–277.
(15) Lakowicz, Y., Jr.; Shen, Y.; Gryczynski, Z.; D'Auria, S.; Gryczynski, I. *Biochem. Biophys. Res. Commun.* **2001**, *286* (5), 875–9.
(16) Matveeva, E.; Gryczynski, Z.; Malicka, J.; Gryczynski, I.; Lakowicz, J. R. *Anal. Biochem.* **2004**, *334* (2), 303–311.
(17) Matveeva, E.; Gryczynski, Z.; Lakowicz, J. R. *J. Immunol. Methods* **2005**, *302* (1−2), 26–35.
(18) Lakowicz, J. R. *Anal. Biochem.* **2005**, *337*, 171–194.
(19) Jacob, J. A.; Mahal, H. S.; Biswas, N.; Mukherjee, T.; Kapoor, S. *Langmuir* **2008**, *24* (2), 528–33.
(20) Shon, Y. S.; Cutler, E. *Langmuir* **2004**, *20* (16), 6626–6630.
(21) Hao, E.; Schatz, G. C.; Hupp, J. T. *J. Fluoresc.* **2004**, *14* (4), 331–341.
(22) Evanoff, D. D., Jr; Chumanov, G. *Chemphyschem.* **2005**, *6* (7), 1221–1231.
(23) Ma, Y.; Li, N.; Yang, C.; Yang, X. *Anal. Bioanal. Chem.* **2005**, *382* (4), 1044–1048.
(24) Panacek, A.; Kvítek, L.; Prucek, R.; Kolar, M.; Vecerova, R.; Pizúrova, N.; Sharma, V. K.; Nevecna, T.; Zboril, R. *J. Phys. Chem. B* **2006**, *110* (33), 16248–16253.
(25) Pan, S.; Wang, Z.; Rothberg, L. J. *J. Phys. Chem. B.* **2006**, *110* (35), 17383–17387.
(26) Ianoul, A.; Bergeron, A *Langmuir* **2006**, *22* (24), 10217–10222.
(27) Cañamares, M. V.; Garcia-Ramos, J. V.; Gómez-Varga, J.D.; Domingo, C.; Sanchez-Cortes, S. *Langmuir* **2007**, *23* (9), 5210–5215.
(28) Pan, S.; Rothberg, L. J. *J. Am. Chem. Soc.* **2005**, *127* (16), 6087–6094.
(29) Krenn, J. R.; Salerno, M.; Felidj, N.; Lamprecht, B.; Schider, G; Leitner, A.; Aussenegg, F. R.; Weeber, J. C.; Dereux, A.; Goudonnet, J. P. *J. Microsc.* **2001**, *202* (Pt 1), 122–8.
(30) Zhang, J.; Matveeva, E.; Gryczynski, I.; Leonenko, Z.; Lakowicz, J. R. *J. Phys. Chem. B.* **2005**, *109* (16), 7969–7975.
(31) Yamaguchi, T.; Kaya, T.; Takei, H. *Anal. Biochem.* **2007**, *364* (2), 171–179.
(32) Ford, G.W.; Weber, W. H. *Phys. Rep.* **1984**, *113*, 195–287.
(33) Das, P.; Metju, H. *J. Phys. Chem.* **1985**, *89*, 4680–4687.
(34) Fleischmann, M.; Hendra, P. J.; McQuillan, A. *J. Chem. Phys. Lett.* **1974**, *26*, 163–170.
(35) Jeanmaire, D. L.; Van Duyne, R. P. *J. Electroanal. Chem. Interface Electrochem.* **1977**, *84*, 1–8.
(36) Lakowicz, J. R. *Principles of Fluorescence. Spectroscopy*, 3rd ed.; Springer: New York, 2006; pp 841−859.
(37) Malicka, J.; Gryczynski, I.; Gryczynski, Z.; Lakowicz, J. R. *Anal. Biochem.* **2003**, *315* (1), 57–66.
(38) Kick, F.; Belitz, H. D.; Wieser, H.; Kieffer, R. Z. *Lebens Unters Forsch.* **1992**, *195*, 437–442.
(39) http://www.setabiomedicals.com/products/K8/K8-1342.pdf
(40) Matveeva, E. G.; Terpetschnig, E. A.; Stevens, M.; Patsenker, L.; Kolosova, O. S.; Gryczynski, Z.; Gryczynski, I. *Dyes Pigm.* **2009**, *80* (1), 41–46.
(41) Varriale, A.; Rossi, M.; Staiano, M.; Terpetschnig, E.; Barbieri, B.; Rossi, M.; D'Auria, S. *Anal Chem* **2007**, *79* (12), 4687–9.
(42) Vader, W.; Kooy, Y.; Van Veelen, P.; De Ru, A.; Harris, D.; Benckhuijsen, W.; Pēna, S.; Mearin, L.; Drijfhout, J. W.; Koning, F. *Gastroenterology* **2002**, *122* (7), 1729–37.
(43) Rumbo, M.; Chirdo, F. G.; Fossati, C. A.; Añón, M. C. *J. Agric. Food*

ARTICLE

Chem. **2001**, *49* (12), 5719–26.
(44) Fan, F.-R. F.; Bard, A. J. *Proc. Natl. Acad. Sci. U.S.A.* **1999**, *96* (25), 14222–14227.
(45) Malicka, J.; Gryczynski, I.; Fang, J.; Lakowicz, J.R. *Anal. Biochem.* **2003**, *317*, 136–146.
(46) Collin, P.; Thorell, T.; Kaukinen, K.; Maki, M. *Aliment. Pharmacol. Ther.* **2004**, *19*, 1277–83.
(47) Catassi, C. I.; Fagiani, E.; Iacono, G.; D'Agate, C.; Francavilla, R.; Biagi, F; Volta, U.; Accomando, S.; Picarelli, A.; De Vitis, I.; Pianella, G.; Gesuita, R.; Carle, F.; Mandolesi, A.; Bearzi, I.; Fasano, A. *Am. J. Clin. Nutr.* **2007**, *85*, 160.
(48) Goldys, E. M.; Drozdowicz-Tomsia, K.; Xie, F.; Shtoyko, T.; Matveeva, E. G.; Gryczynski, I.; Gryczynski, Z. *J. Am. Chem. Soc.* **2007**, *129*, 12117.
(49) Matveeva, E. G.; Chang, I.-F.; Gryczynski, Z.; Goldys, E.; Gryczynski, I.; Shtoyko, T. *Anal. Chem.* **2008**, *80*, 1962–1966.

AM900617P